Seasonal-longitudinal variation of substorm occurrence frequency: Evidence for ionospheric control

H. Wang[1,2] and H. Lühr[3]

Received 22 January 2007; revised 1 March 2007; accepted 9 March 2007; published 7 April 2007.

[1] Based on 2760 well-defined substorm onsets in the northern hemisphere and 1432 in the southern hemisphere observed by the FUV (Far Ultraviolet) Imager on board IMAGE (Imager for Magnetosphere-to-Aurora Global Exploration) spacecraft, a statistical study is performed for both hemispheres. The main emphasis is put on a possible dependence of the substorm occurrence frequency on season and longitude (S/L). It was found that around December solstice UT noon-time and around June solstice UT nighttimes are more favorable for substorms to occur. The occurrence frequency varies by a factor of 2. The sum of ionospheric Pedersen conductances of both hemispheres caused by solar illumination in the nightside auroral regions can account for the S/L dependence. Lower total conductivity seems to reduce the trigger level. We find that the IMF threshold for initiating a substorm is on average lower during favorable times, thus, substorms can occur more frequently. **Citation:** Wang, H., and H. Lühr (2007), Seasonal-longitudinal variation of substorm occurrence frequency: Evidence for ionospheric control, *Geophys. Res. Lett.*, *34*, L07104, doi:10.1029/2007GL029423.

1. Introduction

[2] A substorm onset is regarded as an impulsive unloading of previously stored energy in the magnetospheric tail [e.g., *Rostoker et al.*, 1987; *Baker et al.*, 1996]. The associated precipitation of energetic charged particles marks the conjugate ionospheric footprints of the active magnetotail region. Optical observations of auroral activity are therefore a suitable mean for investigating important properties of a substorm [*Elphinstone et al.*, 1995]. Particularly suitable for that purpose are the global auroral observations of the IMAGE spacecraft. In a dedicated survey auroral break-ups have been identified in the IMAGE-FUV data [*Frey et al.*, 2004; *Frey and Mende*, 2007] including both the northern and southern hemisphere. For the years 2000 through 2005 these authors compiled a list of over 4000 events well distributed over all seasons.

[3] An issue, still under debate, is the main trigger mechanism for a substorm onset. The different underlaying models for internal or external triggers have been discussed elsewhere [e.g., *Lui*, 1996; *Lyons*, 1996; *Shiokawa et al.*, 1998]. In this study we will make use of the large collection of substorm events compiled in the above mentioned list to address some of the open questions in a statistical approach. The advantage of looking at average properties compared to event studies is that several aspects can be considered simultaneously. In particular, we will try to find out the solar wind and interplanetary magnetic field (IMF) configurations preceding the substorm onset and search for conditions which may control the trigger level. This includes the question whether the ionospheric conditions also have a control on the occurrence of a break-up.

[4] In the sections to follow, we first introduce the data set of substorm events and solar wind data used here. Then we present the observed occurrence frequency in a month-by-universal time frame. Finally, we discuss the occurrence distribution in the context of solar wind conditions and ionospheric conductivity.

2. Data Sets

[5] For this study we have made use of the event list of the substorm onset times and locations observed by IMAGE-FUV [*Frey et al.*, 2004; *Frey and Mende*, 2007]. A detailed description of the instrument on board the IMAGE spacecraft and how to determine auroral substorm onsets from the FUV instrument can be found in the work of *Frey et al.* [2004]. In the northern hemisphere the data covers the period from May 2000 (start of the regular IMAGE-FUV operations) through December 2003, while in the south it spans January 2004 to December 2005. The compiled list of substorm onset times and locations covers all seasons quite evenly. For the months April and October in the southern hemisphere and April in the northern hemisphere there are markedly fewer entries in the event list. During these months the camera had to be deactivated for most of the time, in order to protect it against direct sunlight exposure.

[6] In addition, we use 1 min IMF and solar wind velocity data collected by the Advanced Composition Explorer (ACE) satellite. The satellite is located at the Lagrange Points (L1) ~220 RE (~1.48 million km) in front of the Earth. The solar wind data have been propagated from the ACE satellite to the magnetopause (The propagation has been done by the standard procedure and is available at http://nssdc.gsfc.nasa.gov/omniweb/html/omni2_doc.html). The solar wind parameters at the magnetopause are averaged over a 20 min period preceding the time of the onset [*Gérard et al.*, 2004].

3. Observation

[7] The large number of substorm onset events identified with the IMAGE-FUV instrument (2760 northern hemi-

[1]Department of Atmospheric, Oceanic, and Space Science, University of Michigan, Ann Arbor, Michigan, USA.
[2]On leave from College of Electronic Informatics, Wuhan University, Hubei, China.
[3]GeoForschungsZentrum Potsdam, Potsdam, Germany.

0094-8276/07/2007GL029423

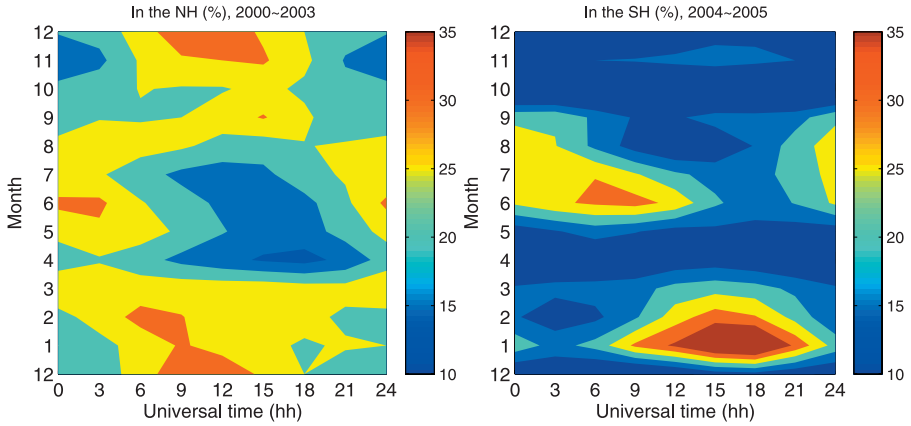

Figure 1. Contour plot of the seasonal variation of the substorm onset occurrence frequency versus UT hours. Color code reflects the probability in percent for a substorm to occur during an hour.

sphere, 1432 southern hemisphere) are a good basis for investigating average conditions associated with a break-up.

3.1. Seasonal Variation of Substorm Occurrence

[8] In this study we are particularly interested in a possible dependence of the substorm occurrence rate on the local seasons in the two hemispheres. Figure 1 shows the distribution of the occurrence frequency in a month versus universal time diagram separately for the northern and southern polar region. There seem to be certain time intervals more favorable for substorms to occur than others. We find a certain concentration during the solstices in the northern hemisphere. In the south the occurrence distribution is similar but delayed by about one month. The reduced rates during April and October are instrumental effects (see section 2). These months are omitted in the following analysis.

[9] The seasonal dependence shows in addition a clear universal time (UT) variation. During December solstice we find many substorms in the northern hemisphere within the time window 0700–1700 UT. Opposed to that around June solstice occurrence rates maximize between 2300–0600 UT. Very similar UT dependencies are found in the southern hemisphere. There are, however, slight shifts of the high occurrence patches to somewhat later hours.

3.2. Seasonal Variation of Merging E-Field

[10] One reason for the variation of the substorm occurrence frequency could be the change in solar wind input. The merging electric field (E_m) has been identified in many studies [e.g., *Troshichev and Lukianova*, 1996; *Ritter et al.*, 2004] as a suitable parameter for describing the solar wind-magnetosphere interaction.

[11] The annual variation of E_m for the years of interest is presented in Figure 2 separately for the intervals when images were taken in the two hemispheres. There is a prominent peak in late fall during both periods. This is a typical feature of the present solar cycle exhibiting strongest magnetic activity in the fall season. The large storm events like the Halloween event and other storms are responsible for the peak of merging electric field in the October 2000–2003 data. Similarly, the severe November 2004 storm causes the peak of the merging electric field in the November 2004–2005 data. The fact that equinoxes are favorable for magnetic activity has alternatively been explained by the solar wind interaction efficiency [e.g., *Temerin and Li*, 2002] or by solar illumination conditions [e.g., *Lyatsky et al.*, 2001]. From a comparison between Figures 1 and 2 we may conclude that this enhanced solar wind input does not lead to an enhanced substorm occurrence rate, and generally, no significant correlation between the depicted quantities can be deduced. In the next section we will try to find an explanation for the variation in occurrence rate.

4. Discussion

[12] The observations presented show that there is a clear dependence of the substorm occurrence rate both on season

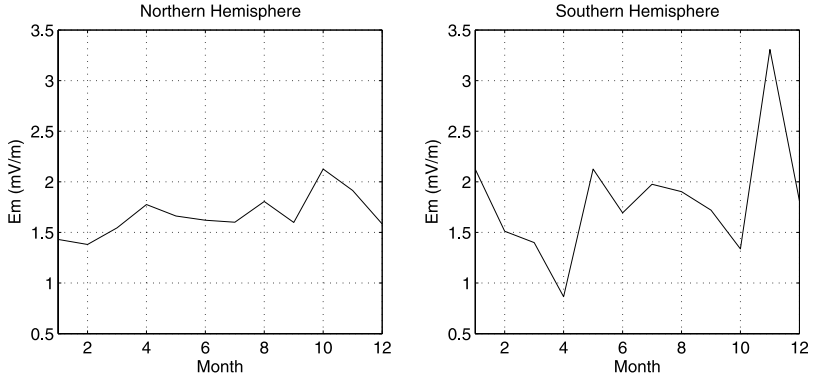

Figure 2. Merging electric field, E_m, as a function of season: (left) Northern Hemisphere observation period and (right) Southern Hemisphere observation period.

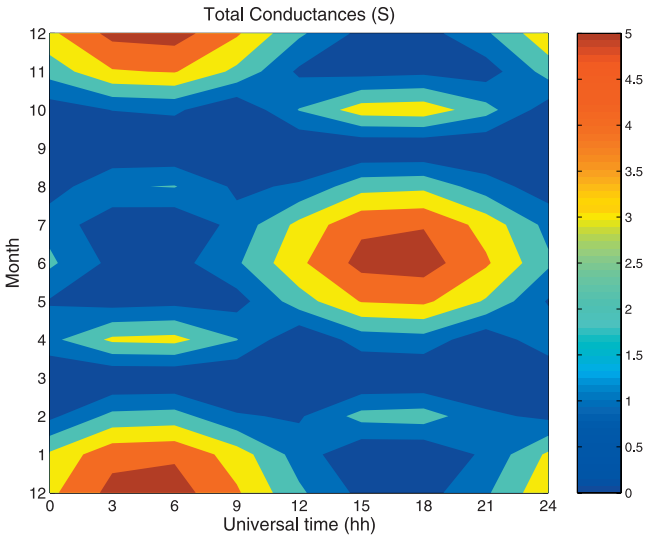

Figure 3. Variation of fluxtube-integrated Pedersen conductances, in S, caused by solar irradiation at the conjugate footprints, ±66.5° MLat and 23 MLT.

and longitude. The rates differ by at least a factor of 2 between minima and maxima. Interestingly, the times of high and low occurrence frequencies are virtually identical in the two hemispheres. This suggests that ionospheric conditions at the conjugate onset sites may play a role.

[13] A quantity we looked at is the ionospheric conductivity caused by solar irradiation. For the estimate of the Pedersen conductance we made use of the approach by *Schlegel* [1988] (for details of computation see *Wang et al.* [2005a]). Since the flux tube on which the onset occurs is connected to both hemispheres, we have plotted in Figure 3 the expected fluxtube-integrated Pedersen conductance for a typical break-up location, ±66.5° MLat at 23 MLT [*Wang et al.*, 2005b].

[14] As expected, conductance maxima appear during the two solstices but at different UTs. When comparing Figures 1 and 3 we find a clear correlation of high substorm occurrence rates at times of low conductance. In particular, the pattern of the southern hemisphere fits well into the conductance gaps.

[15] It seems that a low ionosphere conductance enhances the occurrence rate, thus lowing the threshold for a substorm to be initiated. To test this suggestion we performed a superposed epoch analysis (SPE) with some suitable solar wind parameters. Previous studies have shown that the northward turning of the IMF B_z is a typical trigger for a substorm onset [e.g., *Lyons*, 1996; *Wang et al.*, 2005b], and during times of extended southward IMF dynamic solar wind pressure pulses (either a 50% or 3nPa increase, whatever is lesser) may also trigger a substorm [*Lyons et al.*, 2005]. We divided the event list into two groups depending on the occurrence frequency. All events occurring during the months November 1 through March 31 within the time sector 0900–2100 UT and the months May 1 through September 30 in the sector 2100–0900 UT go into the group 'high rate'. All events occurring during the remaining time are sorted into the 'low rate' group (2098 events in the high rate and 2094 in the low rate group). We did not differentiate between hemispheres since the intervals are the same for both.

[16] Superposed epoch analysis were performed separately for the events of the two groups using their onset times as the key times. The solar wind data used here are from the ACE satellite. They are delayed in time to account for the propagation up to the magnetopause. In Figure 4 the results are shown. Depicted are the average variations of the IMF B_z component and the dynamic pressure during the hours around the onset. The B_z component shows the typical

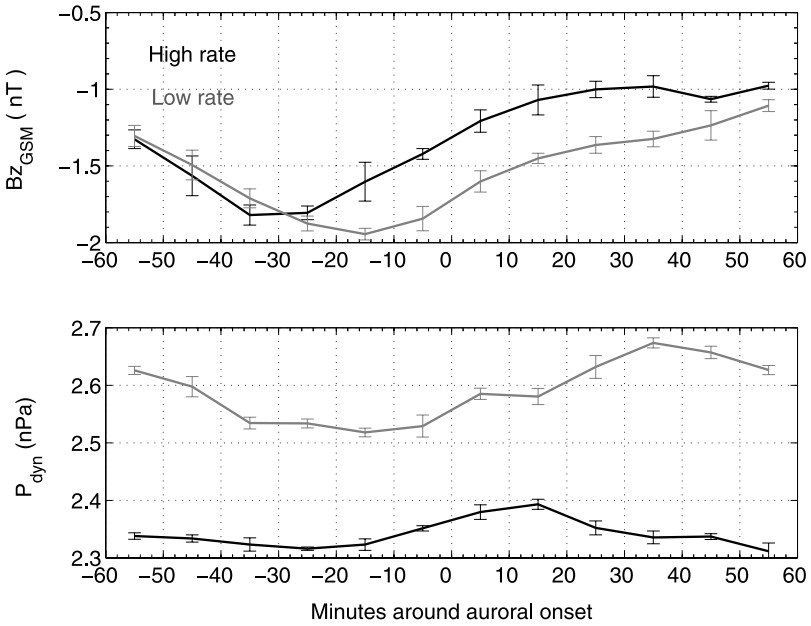

Figure 4. Superposed epoch analysis of solar wind parameters around auroral break-up. The key time, '0', corresponds to the onset time. Parameters are the IMF B_z and solar wind dynamic pressure, P_{dyn}. These quantities have been propagated to the dayside magnetopause. Bars indicate the mean uncertainty of the 10 min averages.

variation, a minimum about 20 min before the onset and a northward turning at the onset time [e.g., *Caan et al.*, 1975; *Wang et al.*, 2005b]. Interestingly, the minimum in B_z is significantly deeper for the 'low rate' events than for the 'high rate' group. Conversely, the dynamic pressure is on average higher before the onset of events in the unfavorable group.

[17] These observations imply that a higher trigger level for substorm onsets exists when the conductance of the associated fluxtube connecting the magnetospheric source region to the ionospheres in both hemispheres is higher. From this it can be concluded that ionospheric conditions have a direct influence on the occurrence of a substorm, the lower the Pedersen conductance of a fluxtube, the easier it is to initiate a substorm.

[18] According to Lyon's model [*Lyons et al.*, 2005], a larger increase in P_{dyn} is required for current wedge formation when preceded by a smaller southward B_z. We find from our analysis that the 'high rate' events are preceded by a weaker southward B_z and lower P_{dyn} enhancement, as the 'low rate' events. The results suggest that the Lyon's model should be extended by another parameter, the fluxtube-integrated Pedersen conductance. For a quantitative description of the ionospheric influence on substorm onset it would be desirable to have besides the solar wind and magnetospheric data also the conductances at the breakup locations in both hemispheres. This may be a suitable research topic for the THEMIS project.

5. Summary

[19] We have found a distinct season/longitude (S/L) dependence of substorm occurrence frequencies equally valid for both hemispheres. The ionospheric conductivity seems to have a significant influence on the trigger level of an onset. Markedly reduced occurrence rates are found if one of the field line footprint regions is in sunlight. The S/L dependence causes a variation in occurrence frequency by about a factor of 2. The dependence on ionospheric conductivity can also be the reason, why pseudo-break-ups are generally observed before midnight and not after. Substorm statistics based on regional measurements are strongly biased by the S/L signature. One such example is the much lower substorm occurrence rate during summer compared to winter in the European sector. Just the opposite tendency would be expected in the Pacific sector.

[20] **Acknowledgments.** We thank H. Frey for making available the IMAGE substorm event list. The ACE data propagated to the magnetopause have kindly been provided by F. Christiansen. This work at University of Michigan was supported by NASA grant F010639 and at Wuhan University by National Nature Science Foundation of China (40604017).

References

Baker, D. N., T. I. Pulkkinen, V. Angelopoulos, W. Baumjohann, and R. L. McPherron (1996), Neutral line model of substorms: Past results and present view, *J. Geophys. Res.*, *101*, 12,975–13,010.

Caan, M. N., R. L. McPherron, and C. T. Russell (1975), Fast auroral snapshot observations of the dependence of dayside auroral field-aligned currents on solar wind parameters and solar illumination, *J. Geophys. Res.*, *80*, 191–194.

Elphinstone, R. D., et al. (1995), Observations in the vicinity of substorm onset: Implications for substorm process, *J. Geophys. Res.*, *100*, 7937–7969.

Frey, H. U., and S. B. Mende (2007), Substorm onset observations by IMAGE-FUV: 2003–2005, in *Proceedings of the Eighth International Conference on Substorms*, edited by M. Syrjäsuo and E. Donovan, Univ. of Calgary, Alberta, Can., in press.

Frey, H. U., S. B. Mende, V. Angelopoulos, and E. F. Donovan (2004), Substorm onset observations by IMAGE-FUV, *J. Geophys. Res.*, *109*, A10304, doi:10.1029/2004JA010607.

Gérard, J.-C., B. Hubert, A. Grard, M. Meurant, and S. B. Mende (2004), Solar wind control of auroral substorm onset locations observed with the IMAGE-FUV imagers, *J. Geophys. Res.*, *109*, A03208, doi:10.1029/2003JA010129.

Lui, A. T. Y. (1996), Current disruption in the Earth's magnetosphere: Observations and models, *J. Geophys. Res.*, *101*, 13,067–13,088.

Lyatsky, W., P. T. Newell, and A. Hamza (2001), Solar illumination as cause of the equinoctial preference for geomagnetic activity, *Geophys. Res. Lett.*, *28*, 2353–2356.

Lyons, L. R. (1996), Substorms: Fundamental observational features, distinction from other disturbances, and external triggering, *J. Geophys. Res.*, *101*, 13,011–13,026.

Lyons, L. R., D. Y. Lee, C. P. Wang, and S. B. Mende (2005), Global auroral responses to abrupt solar wind changes: Dynamic pressure, substorm, and null events, *J. Geophys. Res.*, *110*, A08208, doi:10.1029/2005JA011089.

Ritter, P., H. Lühr, A. Viljanen, and S. Maus (2004), High-latitude ionospheric currents during very quiet times: Their characteristics and predictability, *Ann. Geophys.*, *22*, 2001–2014.

Rostoker, G., S.-I. Akasofu, W. Baumjohann, Y. Kamide, and R. L. McPherron (1987), The roles of direct input of energy from the solar wind and unloading of stored magnetotail energy in driving magnetospheric substorms, *Space Sci. Rev.*, *46*, 93–111.

Schlegel, K. (1988), Auroral zone E-region conductivities during solar minimum derived from EISCAT data, *Ann. Geophys.*, *6*, 129–138.

Shiokawa, K., et al. (1998), High-speed ion flow, substorm current wedge, and multiple Pi2 pulsations, *J. Geophys. Res.*, *103*, 4491–4507.

Temerin, M., and X. Li (2002), A new model for the prediction of *Dst* on the basis of the solar wind, *J. Geophys. Res.*, *107*(A12), 1472, doi:10.1029/2001JA007532.

Troshichev, O. A., and R. Y. Lukianova (1996), Polar cap index (PC) as a proxy for ionospheric electric field in the near-pole region, *Geophys. Res. Lett.*, *27*, 3809–3812.

Wang, H., H. Lühr, and S. Y. Ma (2005a), Solar zenith angle and merging electric field control of field-aligned currents: A statistical study of the southern hemisphere, *J. Geophys. Res.*, *110*, A03306, doi:10.1029/2004JA010530.

Wang, H., H. Lühr, S. Y. Ma, and P. Ritter (2005b), Statistical study of the substorm onset: Its dependence on solar wind parameters and solar illumination, *Ann. Geophys.*, *23*, 2069–2079.

H. Lühr, GeoForschungsZentrum Potsdam, Telegrafenberg, D-14473 Potsdam, Germany. (hluehr@gfz-potsdam.de)

H. Wang, University of Michigan, Ann Arbor, MI 48109, USA. (whui@umich.edu)